

Fundamental Physics Experiments in Space

Timothy J Sumner

Imperial College London

Experiments Using Macroscopic Proof-Masses

- **Gravity-Probe B**
 - Geodetic Effect
 - Lense Thirring Effect
- **STEP**
 - Equivalence Principle
- **GAUGE**
 - Equivalence Principle
 - Spin-coupling
 - $1/r^2$
 - Quantum decoherence
 - Quantum EP
- **MicroScope (μ Scope)**
 - Equivalence Principle
- **LISA Pathfinder**
 - GW demonstrator
- **LISA**
 - GW observatory

Gravity-Probe B

Guide Star
IM Pegasi
(HR 8703)

Frame-dragging Precession
39 milliarcseconds/year
(0.000011 degrees/year)

Geodetic Precession
6,606 milliarcseconds/year
(0.0018 degrees/year)

642 kilometers
(~400 miles)

$$\Omega = \frac{3GM}{2c^2 R^3} (\mathbf{R} \times \mathbf{v}) + \frac{GI}{c^2 R^3} \left[\frac{3\mathbf{R}}{R^2} (\boldsymbol{\omega} \cdot \mathbf{R}) - \boldsymbol{\omega} \right]$$

Geodetic Precession Frame-dragging Precession

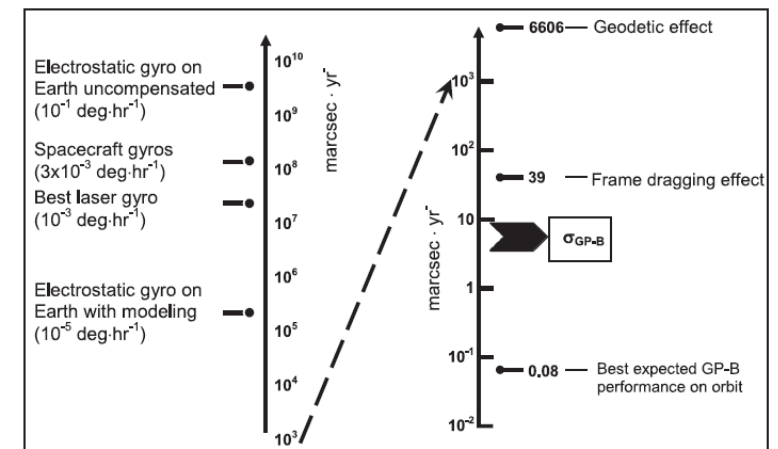
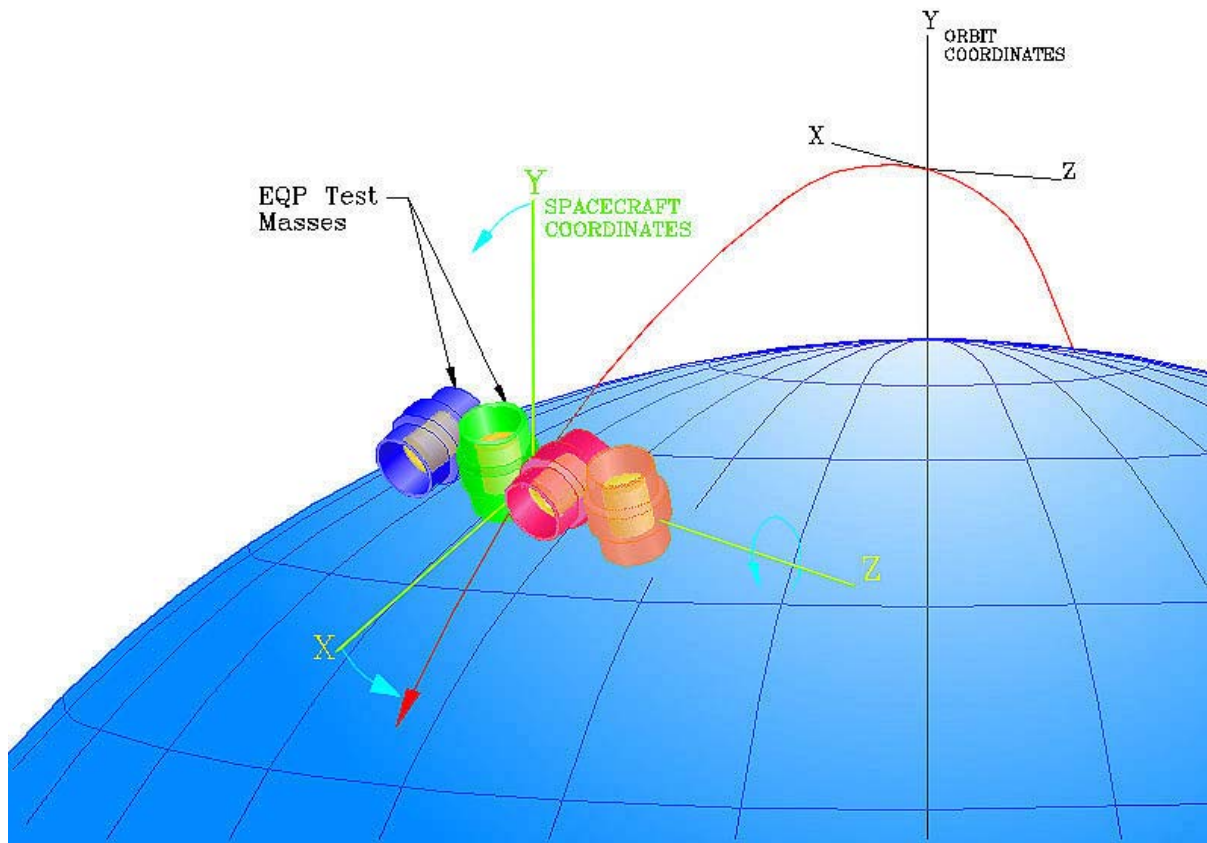


Figure 1. Non-relativistic drift rate of GP-B gyroscopes in space versus ground based gyroscopes. After correction for patch effect torques and modeling of other effects, σ_{GP-B} represents the on-orbit performance achieved by GP-B. 1 marcs = 4.85×10^{-9} radians.

Table 2. Top level requirements on the gyroscopes needed to meet the science goal of the mission.

Gyro parameter		Requirement	Achieved	Verification method
(1)	Rotor mass unbalance tolerance ($\delta r_m/r$)	$\leq 5 \times 10^{-7}$	$\leq 5.1 \times 10^{-7}$	Flight GSS data
(2)	Rotor asphericity ($\delta r_a/r$)	3×10^{-6}	2×10^{-6}	Flight GSS data
(3)	Housing asphericity ($\delta r_H/r_H$)	$\leq 10^{-5}$	$\leq 10^{-5}$	Ground measurement
(4)	Rotor moment of inertia differences	$\leq 10^{-5}$	$\leq 2 \times 10^{-6}$	Flight GSS data
(5)	Rotor spin speed	> 60 Hz	> 61.8 Hz	Flight readout data
(6)	Rotor electric charge	$\leq 10^{-11}$ C	$< 1.3 \times 10^{-11}$ C	Flight GSS charge control
(7)	Operational constraints			
	(a) Rotor spin axis-roll axis angle	< 10 arcsec	< 9.2 arcsec	Flight readout data
	(b) Roll period	$60 \text{ s} < \text{period} < 600 \text{ s}$	77.5 s	Flight roll sensor data
	(c) Rotor mass center to roll axis distance	$< 100 \mu\text{m}$	$< 100 \mu\text{m}$	By design
	(d) Transverse acceleration	$\leq 10^{-10} \text{ m s}^{-2}$	$< 4 \times 10^{-11} \text{ m s}^{-2}$	Flight GSS data
	(e) Orbit plane to guide star angle	$< 0.02^\circ$	$< 0.02^\circ$	Flight GPS data
(8)	Environmental constraints			
	(a) Magnetic field	$\leq 9 \times 10^{-10} \text{ T}$	$\leq 3.1 \times 10^{-10} \text{ T}$	Rotor trapped magnetic flux
	(b) Gas pressure	$\leq 2.6 \times 10^{-8} \text{ Pa}$	$< 2 \times 10^{-12} \text{ Pa}$	Gyro spin down rate

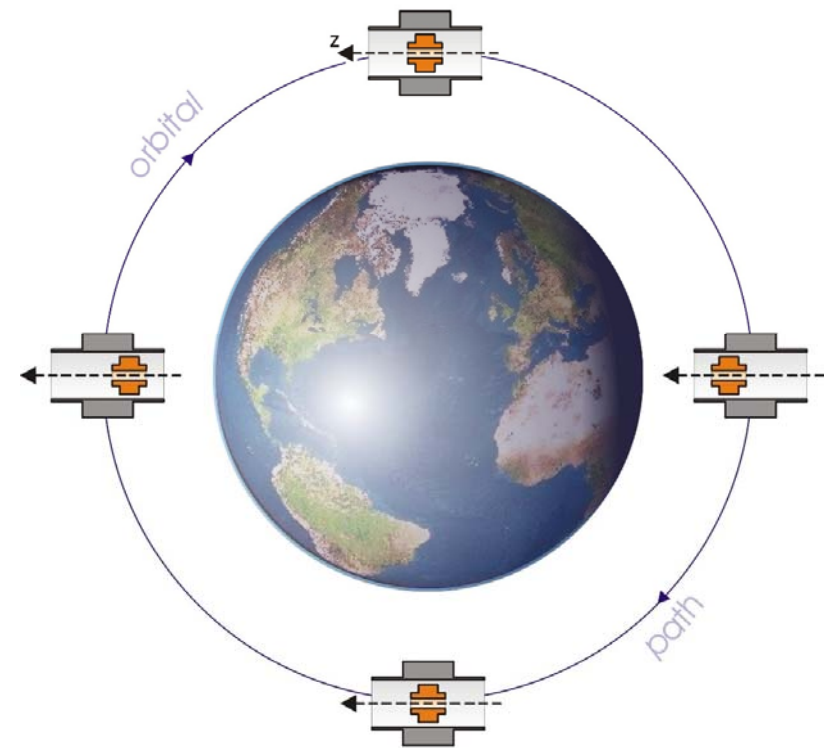
STEP (Satellite Test of the Equivalence Principle)



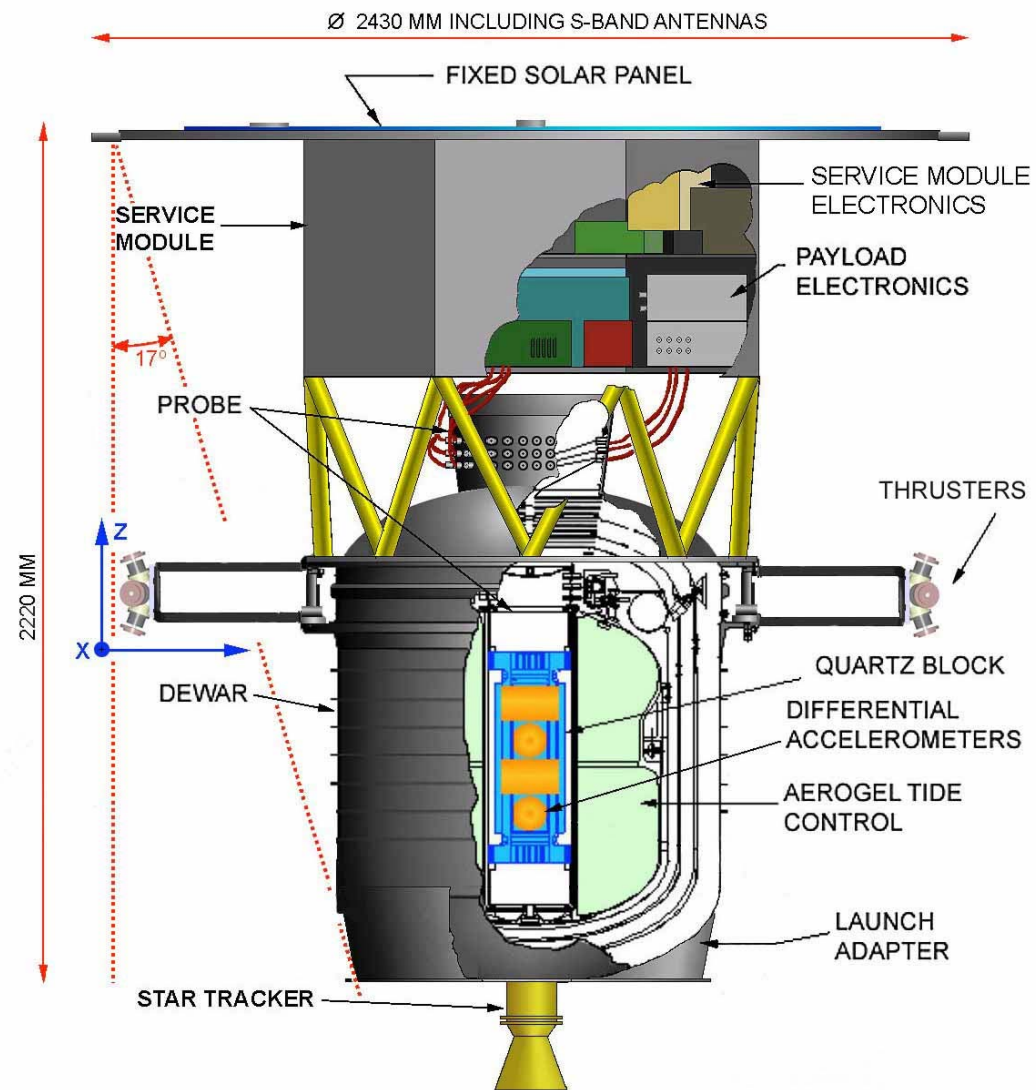
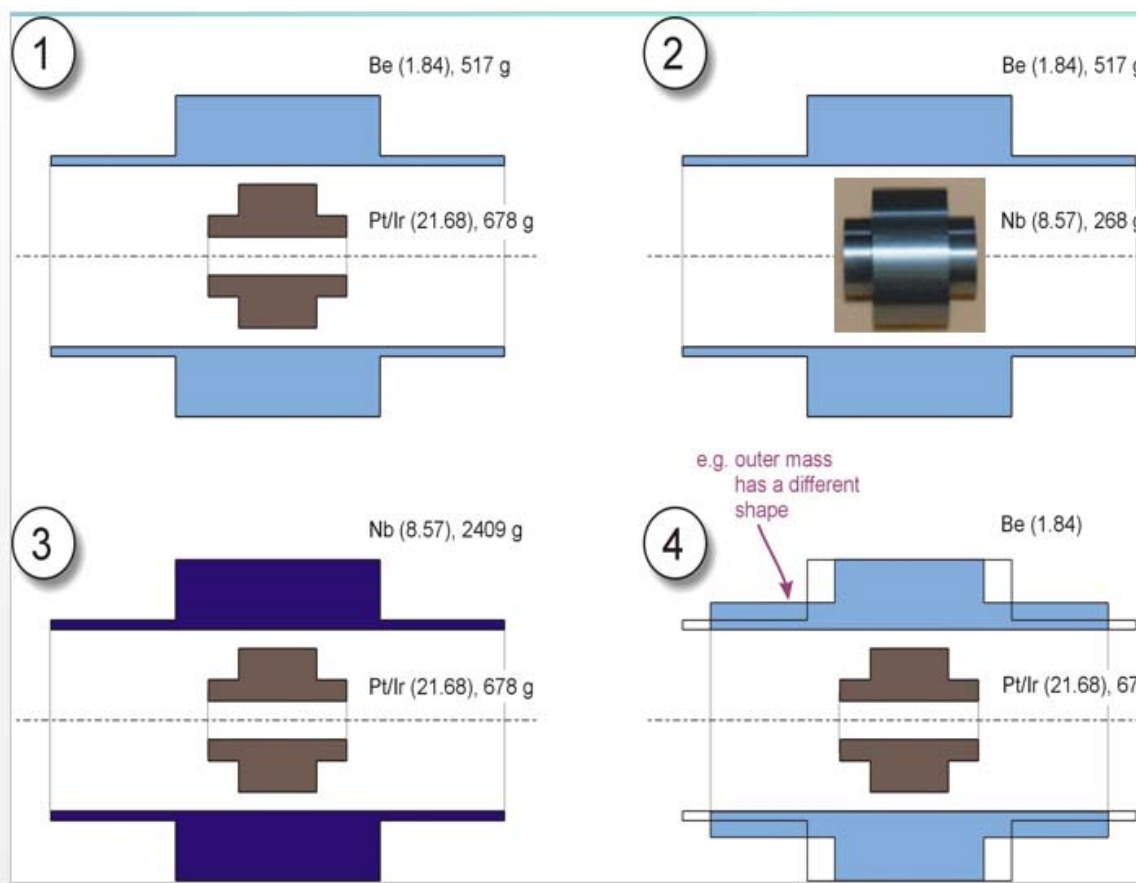
QTSpace, 26-31 Mar 2017, Malta

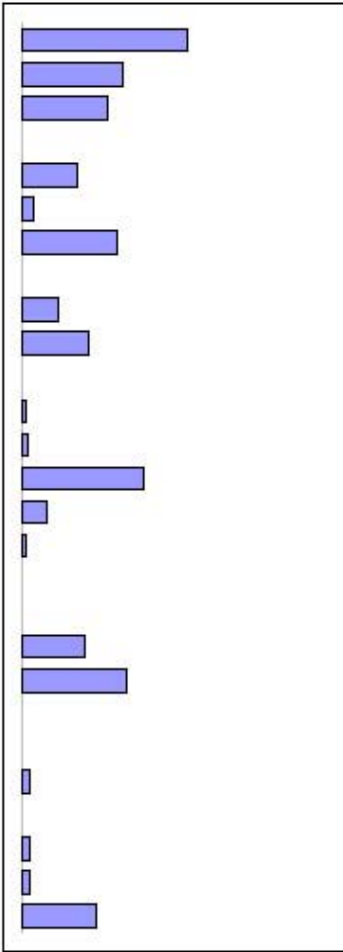
STEP

SATELLITE TEST OF THE EQUIVALENCE PRINCIPLE

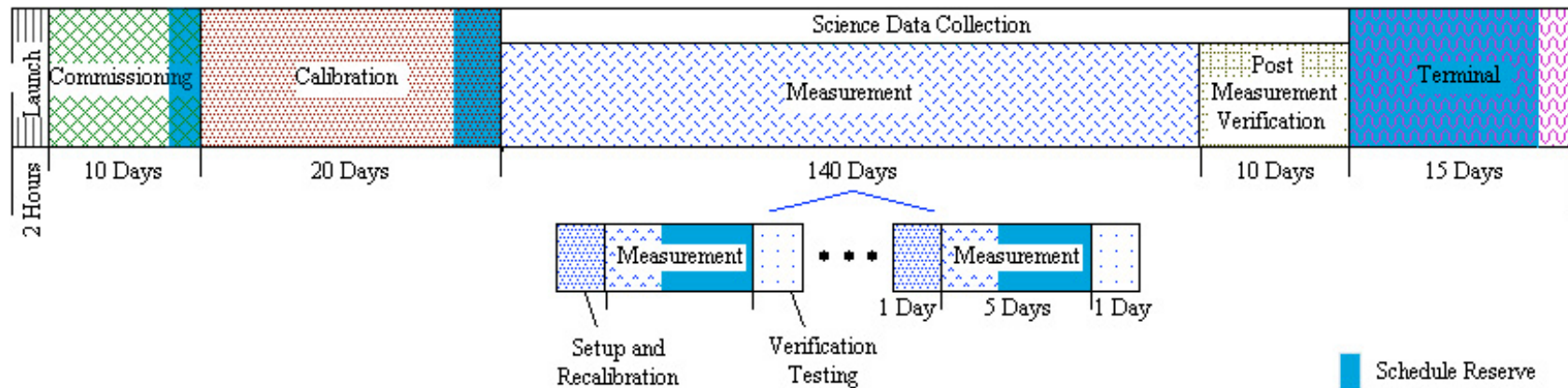


$$\frac{\Delta a_z}{a} = 10^{-18}$$



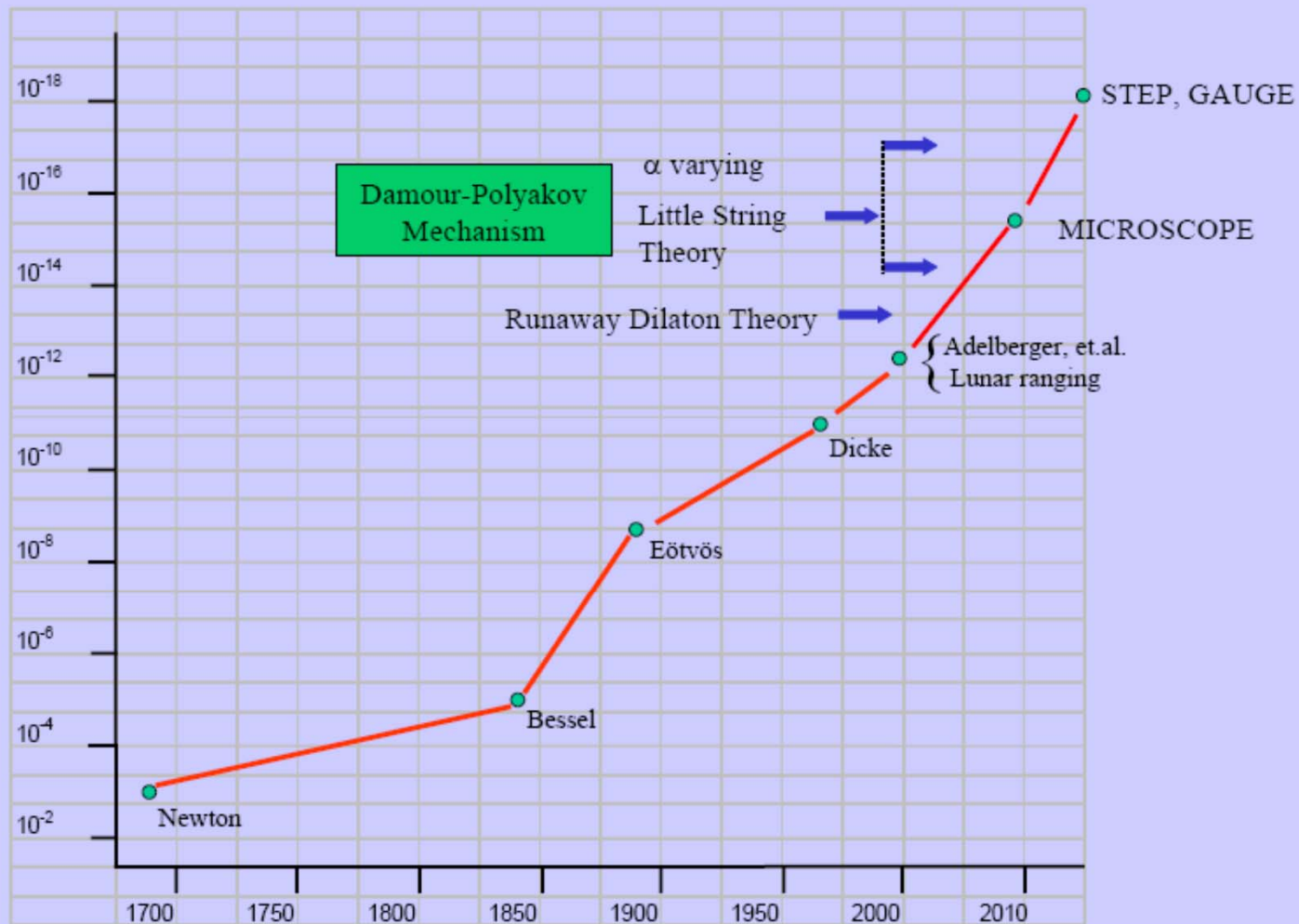
DFC Reference accelerometer Disturbance	Systematic component at signal frequency m/sec^2		Comment
SQUID noise	1.57E-18		acceleration equivalent to intrinsic noise
SQUID temp. drift	9.58E-19		regulation of SQUID carriers
Thermal expansion	8.16E-19		gradient along DAC structure
Differential Thermal expansion	5.07E-23		Radial gradient in DAC structure
Nyquist Noise	5.23E-19		RMS acceleration equivalent
Gas Streaming	1.09E-19		decaying Gas flow, outgassing
Radiometer Effect	8.99E-19		gradient along DAC structure
Thermal radiation on mass	1.86E-22		Radiation pressure, gradient
Var. Discharge uv light	3.48E-19		unstable source, opposite angles on masses
Earth field leakage to SQUID	6.34E-19		estimate for signal frequency component
Earth Field force	4.16E-22		estimate for signal frequency component
Penetration depth change	3.38E-20		longitudinal gradient
Electric Charge	6.22E-20		Assumptions about rate
Electric Potential	1.16E-18		variations in measurement voltage
Sense voltage offset	2.38E-19		bias offset
Drag free residual in diff. Mode	3.91E-20		estimated from squid noise
Viscous coupling	1.84E-23		gas drag + damping
Cosmic ray momentum	3.33E-21		mostly directed downward
Proton radiation momentum	6.03E-19		unidirectional, downward
dynamic CM offset	9.87E-19		vibration about setpoint, converted
static CM offset limit	1.86E-21		A/D saturation by 2nd harmonic gg
Trapped flux drift acceleration	7.37E-23		actual force from Internal field stability
Trapped flux changes in squid	7.12E-20		apparent motion from internal field stability
S/C gradient + CM offset	5.79E-33		gravity gradient coupling to DFC residual of S/C
rotation stability	7.19E-20		centrifugal force variation + offset from axis
Eccentricity subharmonic.	8.17E-20		real part at signal frequency
Helium Tide	7.00E-19		Fixed Placeholder
position sensor gap, mm	1.00		500000 Orbit height
common mode period	1466		0.0086 Sensor current, A
differential mode period	1131		1.6E-11 CM distance, m
S/C rotation per orbit	2.70E+00		
Total error	9.21E-18	RMS error	2.90E-18 m/sec^2

Mission Timeline



- Operational life: 6 months
- 30 days Commissioning and Calibration
- 140 days Measurement - 20, 7 day experiment set-ups
- Each experiment has 4x20 orbit runs sufficient to reach 10^{-18} , multiple measurements improve robustness of data, enable search for systematic effects (some in real-time)
- Post Measurement Verification: non-mission critical measurements that further increase robustness of data
 - e.g. Operation near instabilities, irreversible systematic checks

Space > 5 orders of magnitude leap



GAUGE (GrAnd Unification and Gravity Explorer)

GAUGE (GrAnd Unification and Gravity Explorer) was a proposal in 2007 to the Cosmic Visions programme at ESA. The proposal was for a drag-free spacecraft platform onto which is attached a number of modular experiments, including both **macroscopic** and **microscopic (AI)** proof-masses. The complement of experiments addressed key issues at the interface between gravity and unification with the other forces of nature.

We included:

- ☐ High-precision **macroscopic EP experiment**
- ☐ Quantum space-time fluctuations in a **microscopic EP experiment**
- ☐ An inverse square law test at **intermediate** and **short** ranges
- ☐ An axion-like mass-spin coupling search at **intermediate** and **short** ranges
- ☐ Quantum decoherence from space-time fluctuations **at the Planck scale**

G Amelino-Camelia, K Aplin, M Arndt, J D Barrow, R J Bingham, C Borde, P Bouyer, M Caldwell, A M Cruise, T Damour, P D'Arrigo, H Dittus, W Ertmer, B Foulon, P Gill, G D Hammond, J Hough, C Jentsch, U Johann, P Jetzer, H Klein, A Lambrecht, B Lamine, C Lämmerzahl, N Lockerbie, F Loeffler, J T Mendonca, J Mester, W-T Ni, C Pegrum, A Peters, E Rasel, S Reynaud, D Shaul, T J Sumner, S Theil, C Torrie, P Touboul, C Trenkel, S Vitale, W. Vodel, C Wang, H Ward, A Woodgate

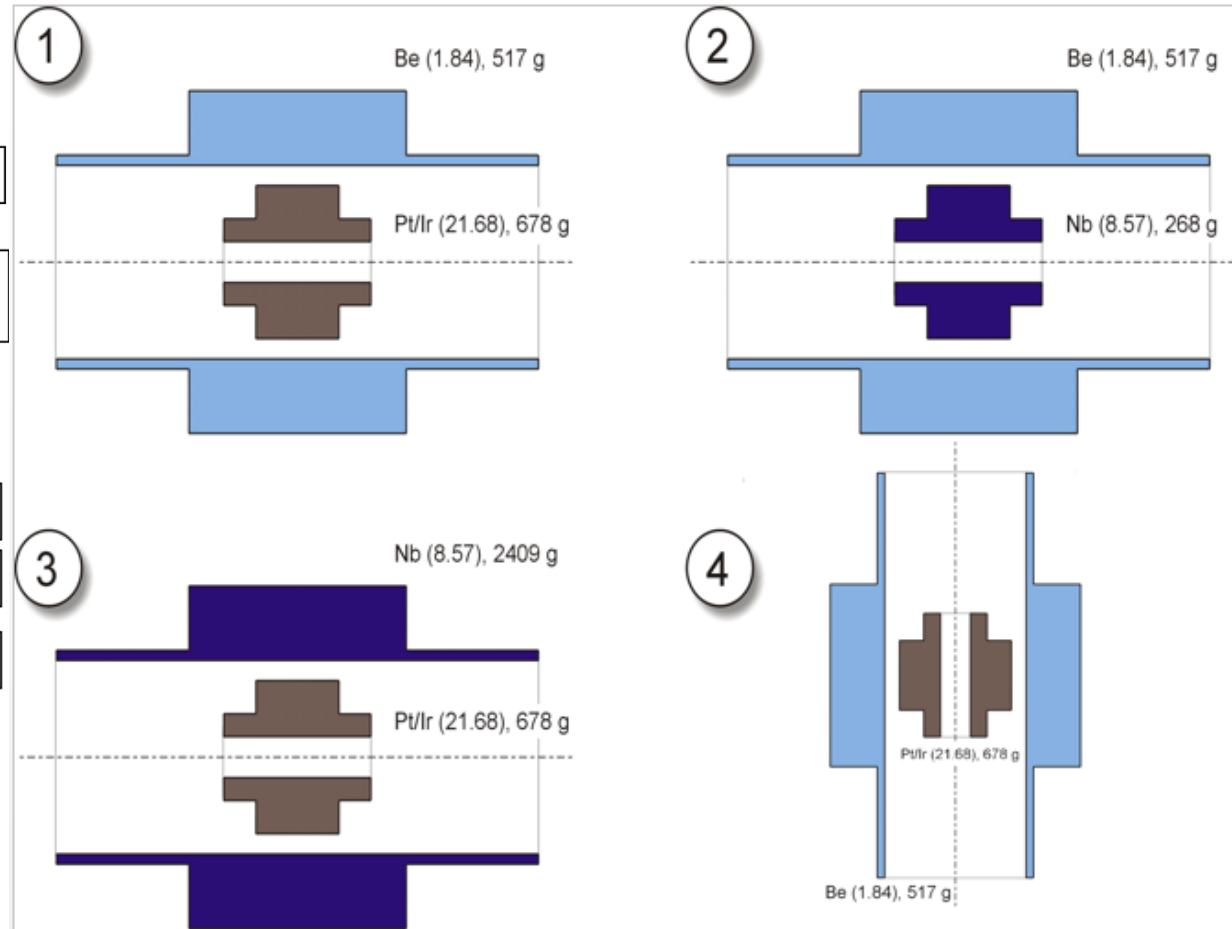
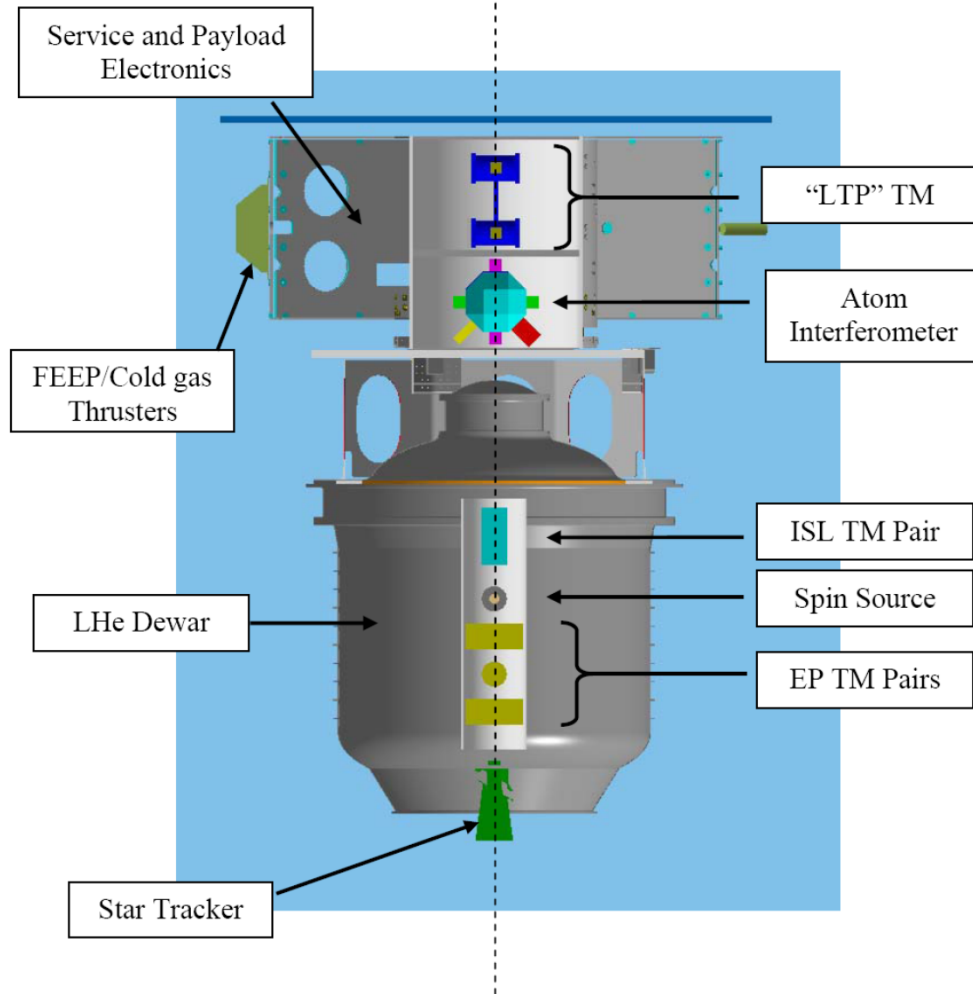
GAUGE

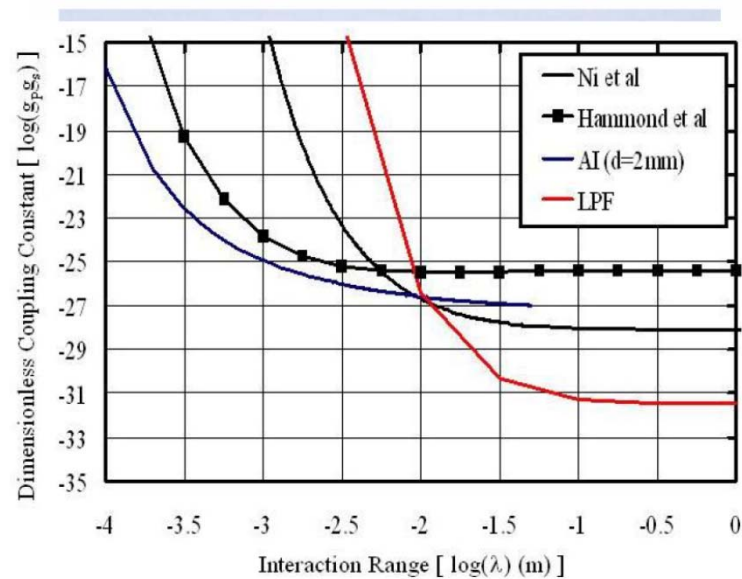
GrAnd Unification and Gravity Explorer

Academics – Experimental – Classical and Quantum
Academics – Theorists
Industry – Space
Government Laboratories

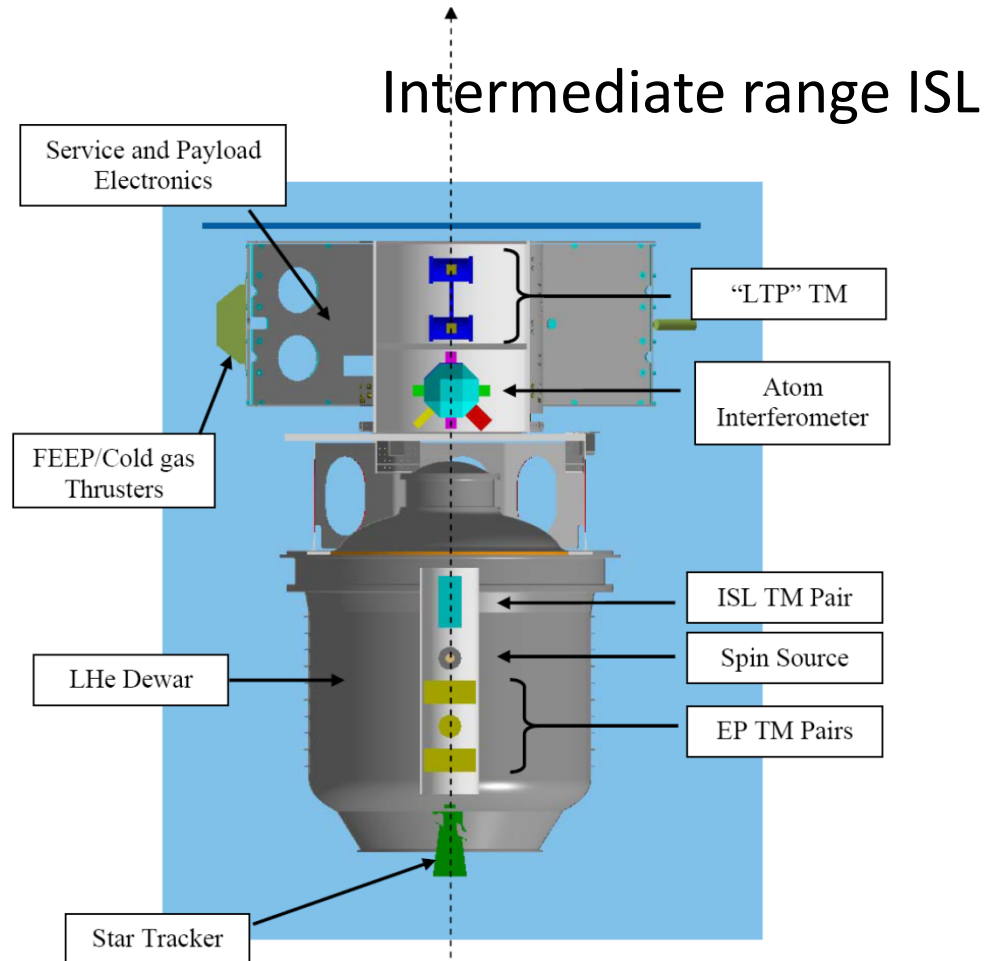
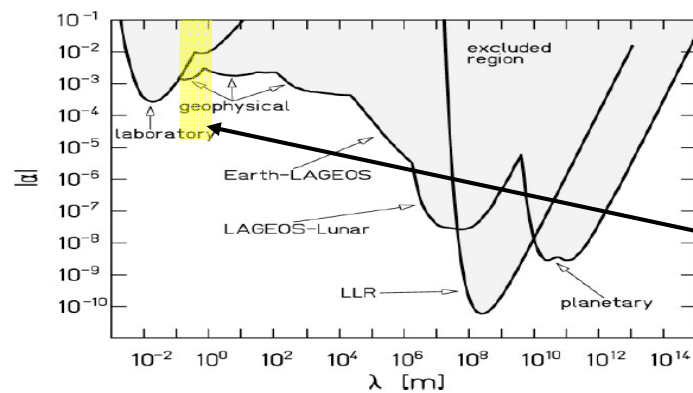
QTSpace, 26-31 Mar 2017, Malta

Macroscopic EP \uparrow





Current limits on anomalous Yukawa terms (Adelberger 2003):



On-board (LTP-GAUGE)

-31 Mar 2017, Malta

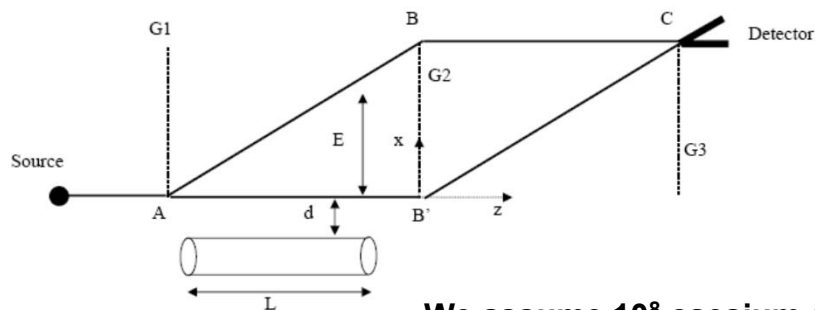
Experiment concepts

- Atom Interferometry

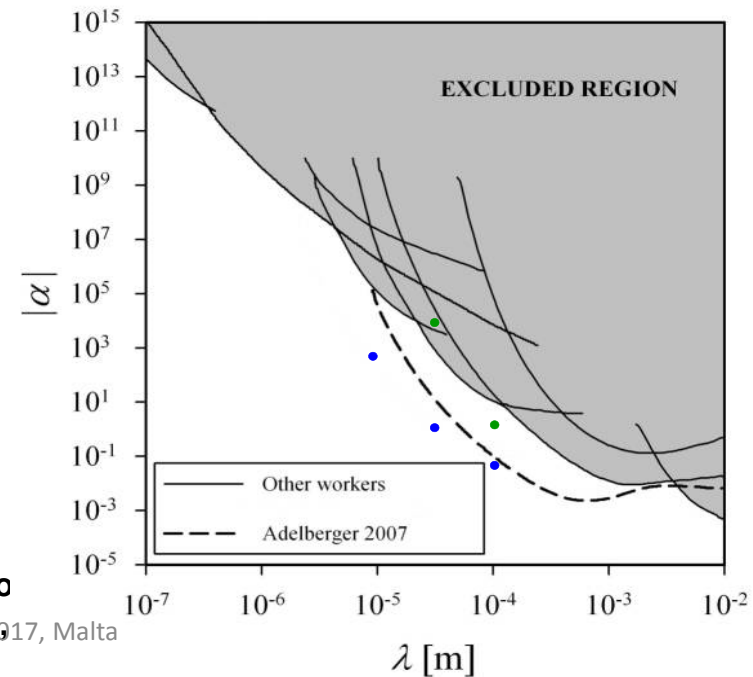
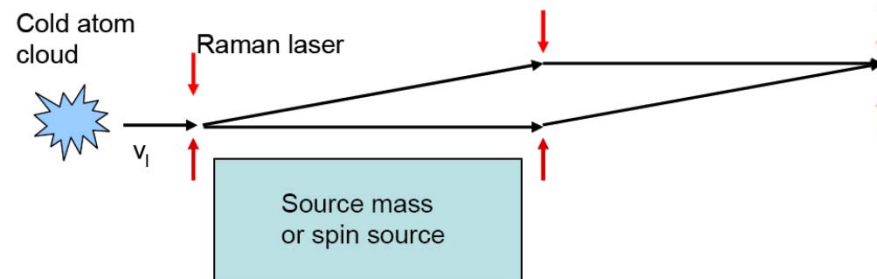
$$V = -\frac{GMm}{r} \left[1 + \alpha e^{-r/\lambda} \right]$$

$$\delta\phi = \frac{1}{\hbar} \int_{ABCB'A} \frac{dr}{v} V(r)$$

Inverse Square Law



We assume 10^8 caesium atoms
effective temperature $\sim 1 \mu\text{K}$
gold.

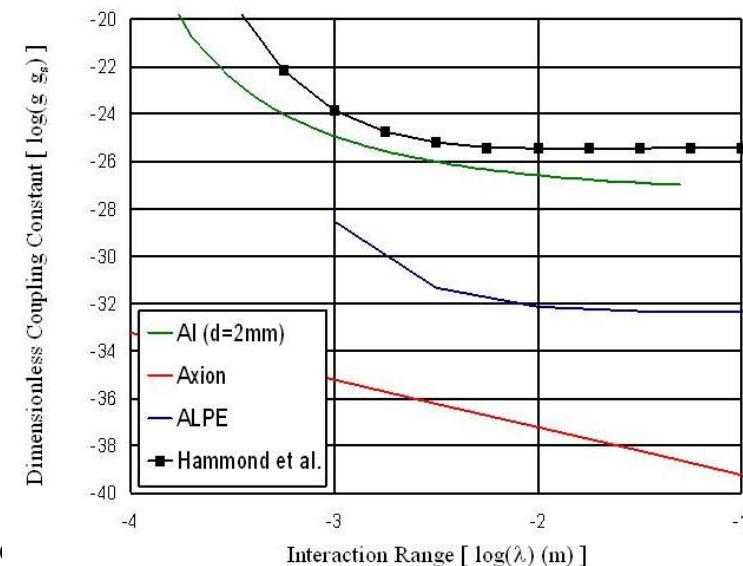
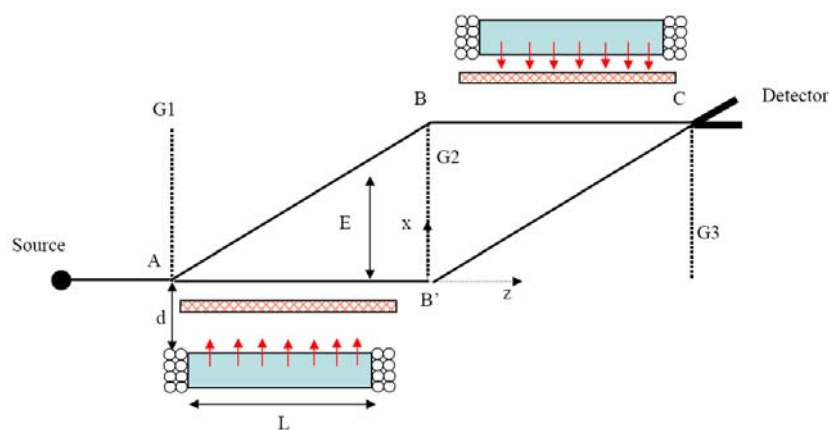
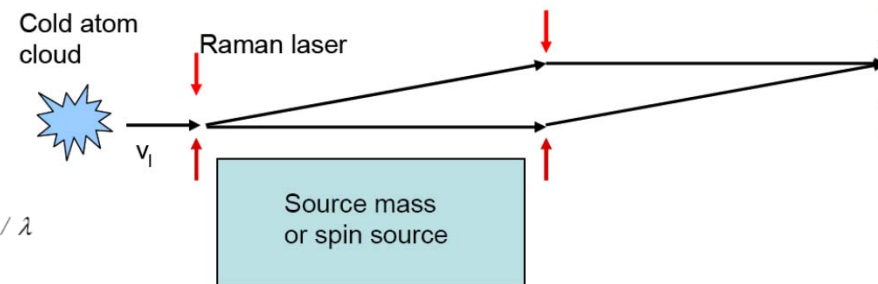


Experiment concepts

- Atom Interferometry

Spin Coupling

$$V(r) = g_p g_s \frac{\hbar^2}{8\pi m_{spin}} \vec{\sigma} \cdot \hat{r} \left(\frac{1}{\lambda r} + \frac{1}{r^2} \right) e^{-r/\lambda}$$

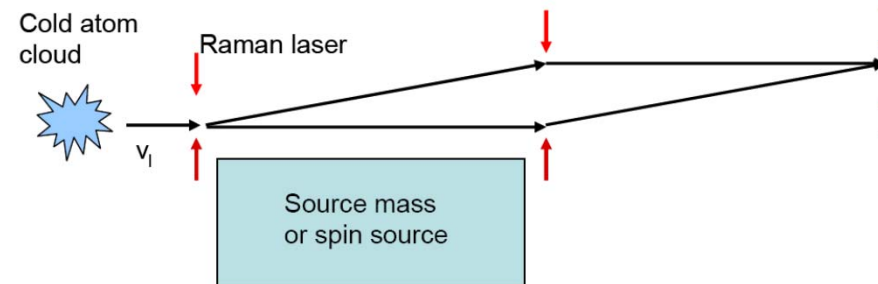


We assume 10^8 caesium at effective temperature $\sim 1\mu\text{K}$, and a source mass of 25cm length made from gold.

Experiment concepts

- Atom Interferometry

Equivalence Principle



Violation of weak equivalence principle (WEP)

For every particle p the ratio of gravitational and inertial mass becomes different, namely

$$\left(\frac{m_g}{m_i}\right)_p = 1 + \alpha_i(\Delta t_p), \quad \alpha_j(\Delta t_p) = \sum_{j=1}^3 \langle \langle \tilde{h}^{ij} \rangle \rangle \Delta t_p$$

→ Violation of the Universality of Free Fall.

Space-Time Fluctuations and Inertia

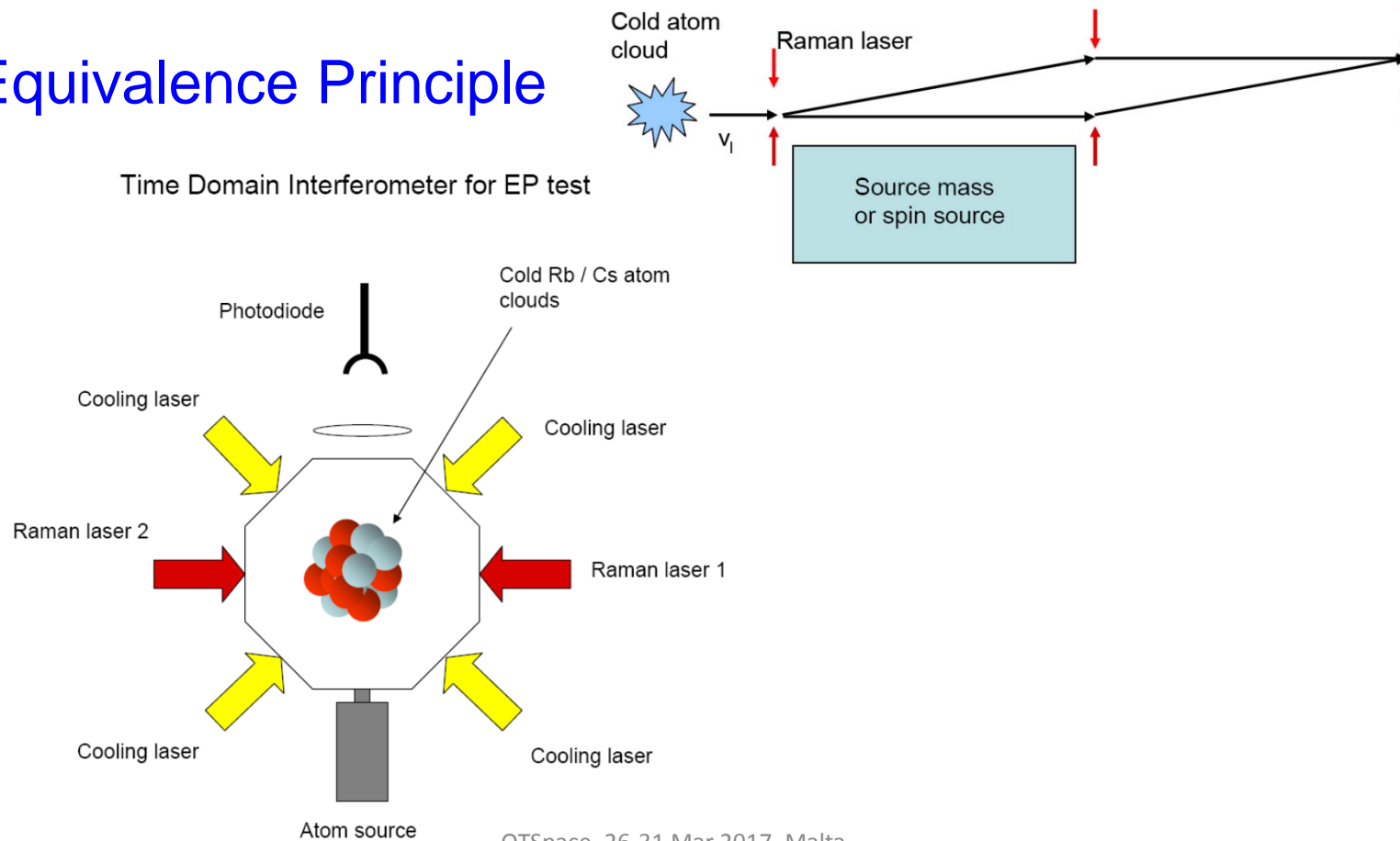
Claus Lämmerzahl and Ertan Göklü

$$\alpha_1 = \frac{10^{-40}}{10^{-26}} = 10^{-14} \quad \text{for Caesium}$$

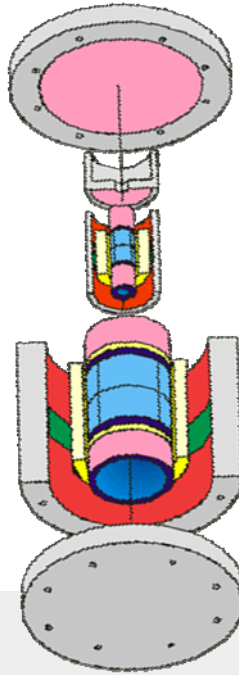
Experiment concepts

- Atom Interferometry

Equivalence Principle

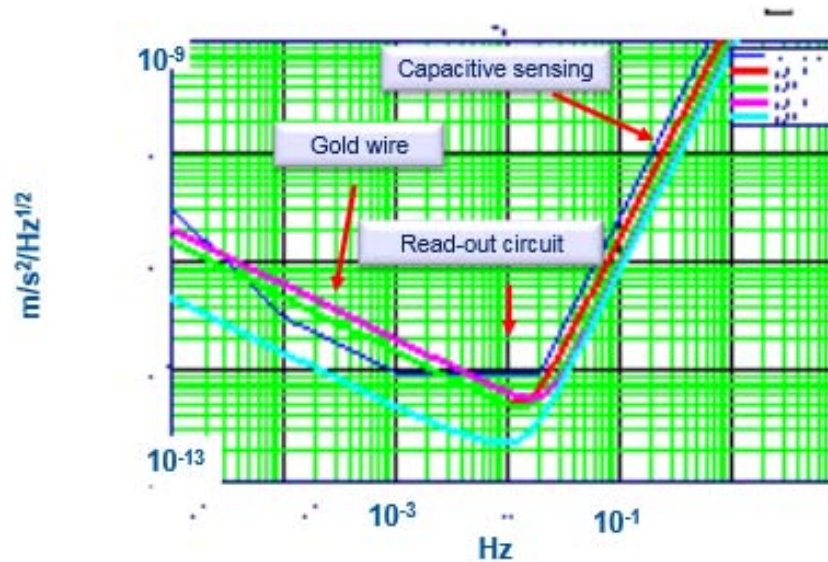


MICROSCOPE (MICROSatellite à trainée Compensée pour l'Observation du Principe d'Équivalence)



- Total mass of the instrument: 50 kg
- Test masses:
 - inside in Platinum = 0.5 kg
 - outside in Platinum = 1.4 kg
 - outside in Titanium = 0.3 kg
- Resolution of the acceleration measurement = $0.1 \text{ pico-g} / \text{Hz}^{1/2}$ in the range $[10^{-3} \text{ Hz} - 2 \times 10^{-2} \text{ Hz}]$

FM error budgets

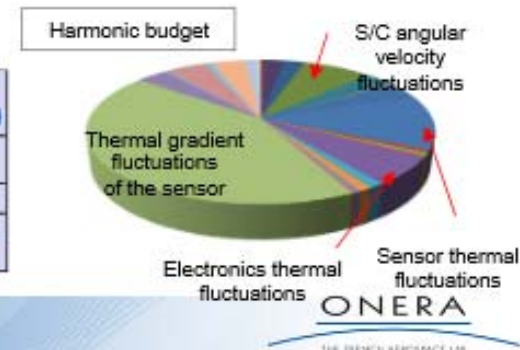


Similar to GOCE sensor noise performance :
demonstrated in orbit by a factor 2 at least in the
[5, 10⁻³; 10⁻¹] bandwidth
MICROSCOPE at lower frequency, smaller
bandwidth and longer integrating period

Overall mission error budget :

- 59 disturbing sources evaluation stochastic & tone
- Instrument : more than 100 contributions
- Taking into account verified instrument and satellite characteristics

	stochastic disturbing source	tone disturbing source	EP (120 orbits)	EP (240 orbits)	EP (360 orbits)
	ms ⁻² /Hz ^{1/2} quadratic sum	ms ⁻² direct sum/3			
Inertial satellite pointing ($f_{sp} = f_{orb} = 1,7 \cdot 10^{-4}$ Hz)	$6,64 \cdot 10^{-11}$	$7,58 \cdot 10^{-18}$	$1,38 \cdot 10^{-18}$	$1,19 \cdot 10^{-18}$	
Rotating satellite attitude ($f_{ra} = 11/2$ or $11/2 f_{orb} = 7,7$ or $9,4 \cdot 10^{-4}$ Hz)	$6,64 \cdot 10^{-12}$	$6,64 \cdot 10^{-18}$	$0,53 \cdot 10^{-18}$	$0,48 \cdot 10^{-18}$	$0,45 \cdot 10^{-19}$



at mission level

Earth Gravity Gradient →	eccentricity $< 5 \cdot 10^{-3}$ S/C position tracking (Doppler) : $< 7m, < 14m, 100m @ fep$ Pointing : 10^{-3} rad with variations $< 10 \mu rad$ (inertial) & $10 \mu rad$ (spin) @ fep
Mass Off-Centering →	Angular velocity variations $< 10^{-9}$ rad/s (spin) @ fep Angular accelerations variations $< 10^{-11}$ rad/s ² (inertial) & $5 \cdot 10^{-12}$ rad/s ² (spin) @ fep
Sensitivity Matching →	Drag-Free Control $< 3 \cdot 10^{-10} ms^{-2} Hz^{-1/2}$ and $< 10^{-12} ms^{-2}$ variations @ fep

Instrument characteristics and in-orbit calibration :

- Resolution : $< 2.3 \cdot 10^{-12} ms^{-2} Hz^{-1/2}$ and $2.6 \cdot 10^{-9} rads^{-2} Hz^{-1/2}$
- Sensitivity stability $< 6.8 \cdot 10^{-8}$ sine (FEEU thermal effect) and $1.2 \cdot 10^{-5} Hz^{-1/2} @ fep$
- SF matching : $< 1.5 \cdot 10^{-4}$
- with stability : $< 0.3 \cdot 10^{-8}$ sine (SU thermal effect) and $3 \cdot 10^{-6} Hz^{-1/2} @ fep$
- Alignment matching* : $< 5 \cdot 10^{-5}$ rad
- with stability : $< 1.5 \cdot 10^{-9}$ rad sine (SU thermal effect) and $3 \cdot 10^{-7} rad Hz^{-1/2} @ fep$

P. Touboul, Space Sci Rev, 2009.

at instrument level

Capacitive sensing :

	Internal Mass (1,4 kg)	External Mass (0,4kg)
X	$12 \mu\text{VHz}^{-1/2} = 4 \cdot 10^{-11} \text{ mHz}^{-1/2}$	$6 \mu\text{VHz}^{-1/2} = 2.5 \cdot 10^{-11} \text{ mHz}^{-1/2}$
Y,Z	$6 \mu\text{VHz}^{-1/2} = 2.5 \cdot 10^{-11} \text{ mHz}^{-1/2}$	$3 \mu\text{VHz}^{-1/2} = 1 \cdot 10^{-11} \text{ mHz}^{-1/2}$

Electrostatic control & measurement :

	Internal Mass	External Mass
X	$1.1 \mu\text{VHz}^{-1/2} = 20 \cdot 10^{-15} \text{ NHZ}^{-1/2}$	$1.6 \mu\text{VHz}^{-1/2} = 52 \cdot 10^{-15} \text{ NHZ}^{-1/2}$
Y,Z	$2.3 \mu\text{VHz}^{-1/2} = 160 \cdot 10^{-15} \text{ NHZ}^{-1/2}$	$2.3 \mu\text{VHz}^{-1/2} = 710 \cdot 10^{-15} \text{ NHZ}^{-1/2}$

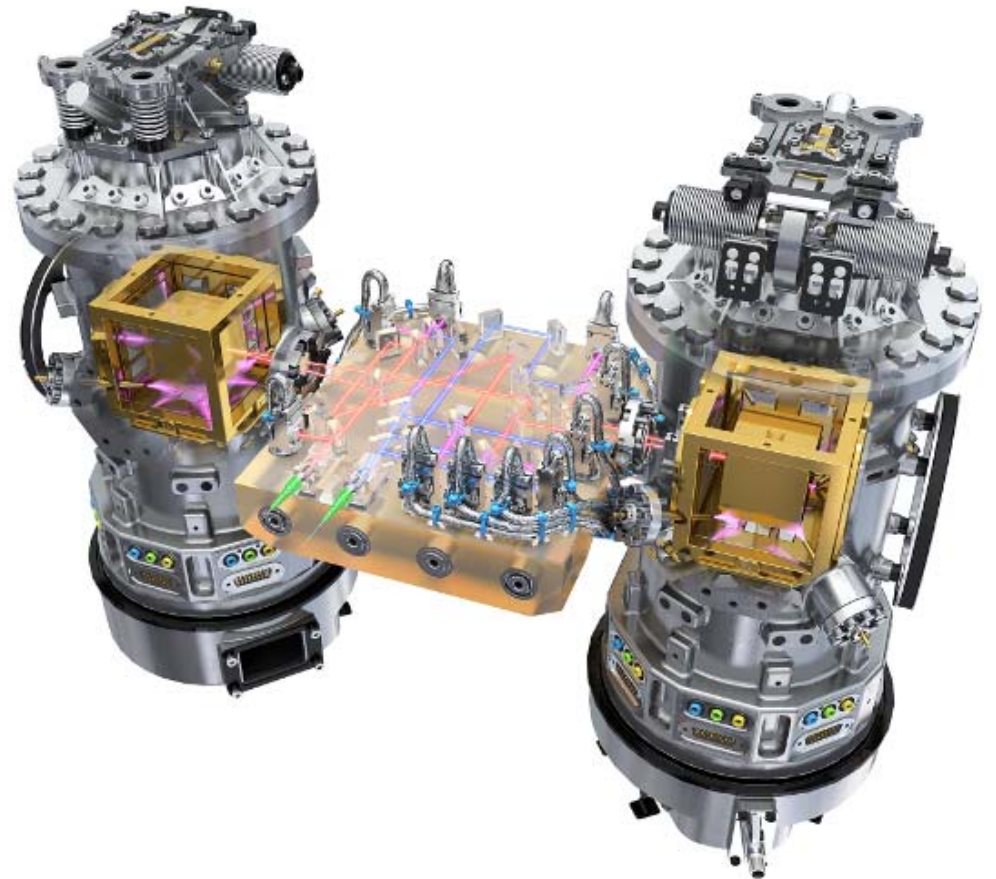
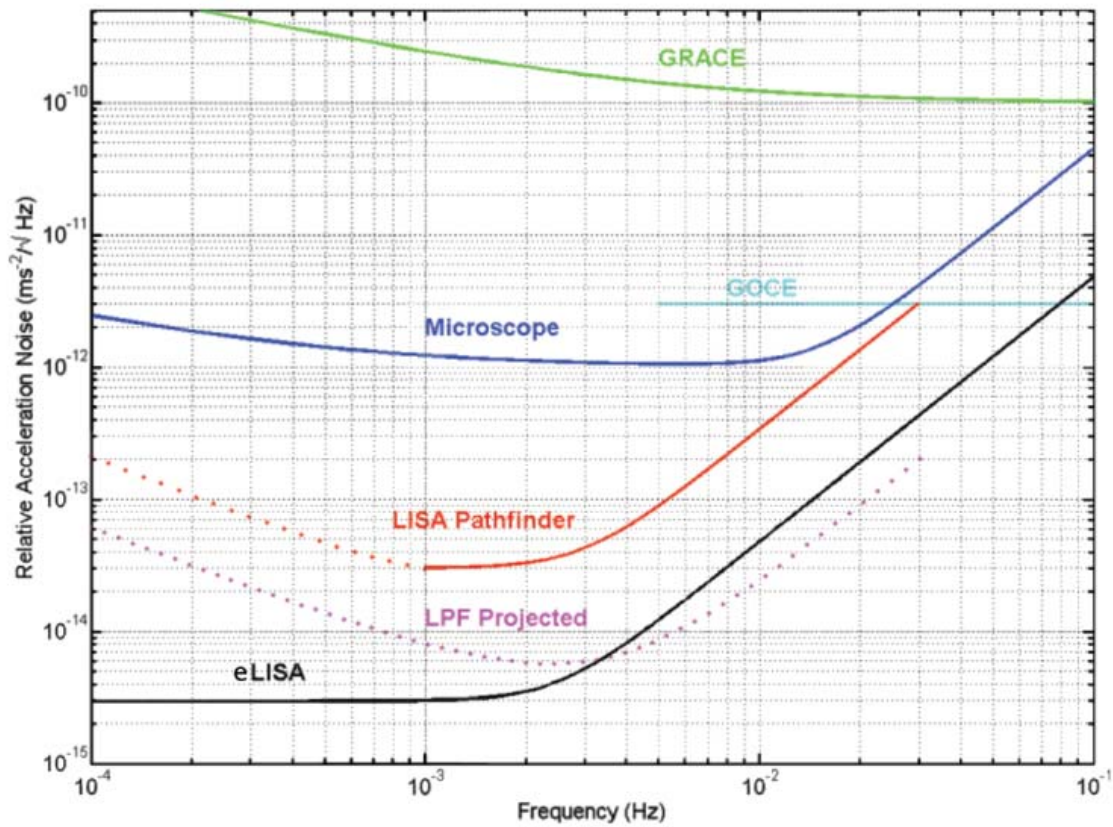
Proof mass reference voltage :

$V_p = 5V$; $0.22 \mu\text{VHz}^{-1/2}$; 13 ppm/°C + stability compatible with 5mK fluctuations

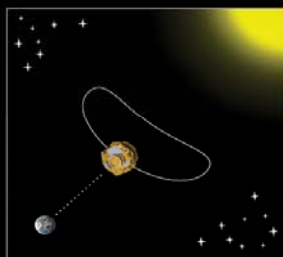
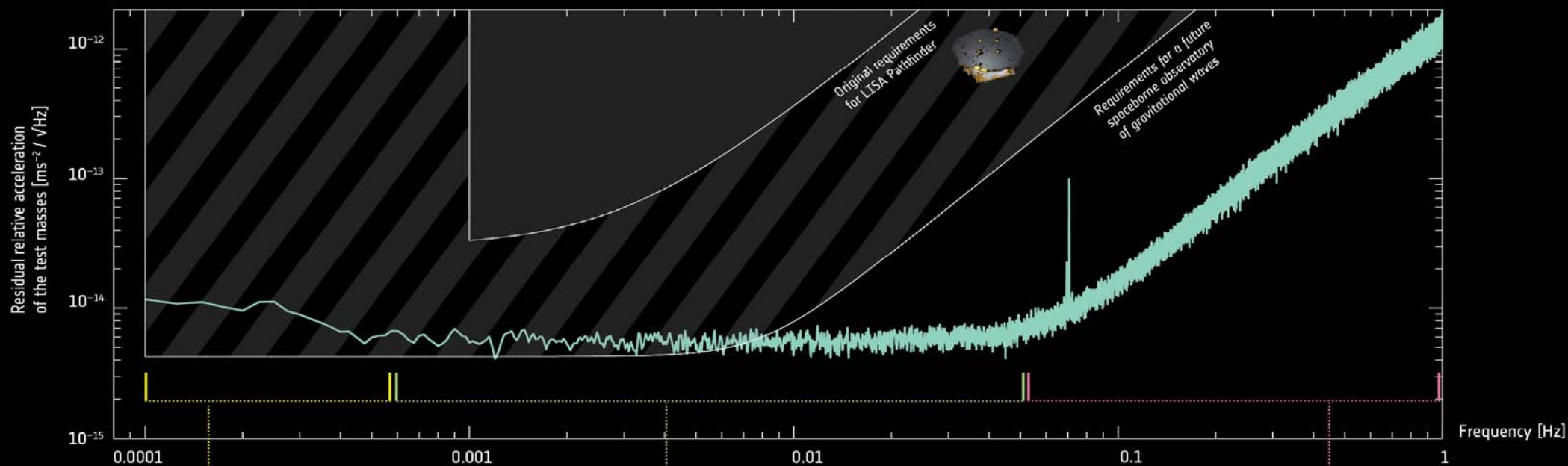
Power supply :

0,1 mV for 1 V satellite power bus variation & 2mV/°C

LISA Pathfinder (LISA Technology Demonstrator)

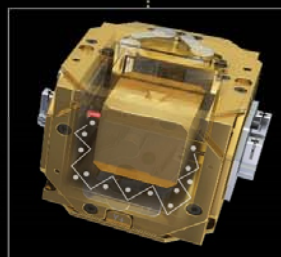


→ LISA PATHFINDER EXCEEDS EXPECTATIONS



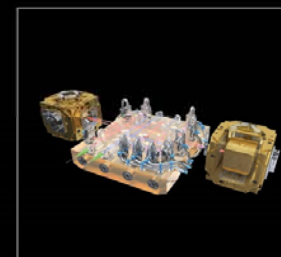
Centrifugal force

The rotation of the spacecraft required to keep the solar array pointed at the Sun and the antenna pointed towards Earth, coupled with the noise of the star trackers produces a noisy centrifugal force on the test masses. This noise term has been subtracted, and the source of the residual noise after subtraction is still being investigated.



Gas damping

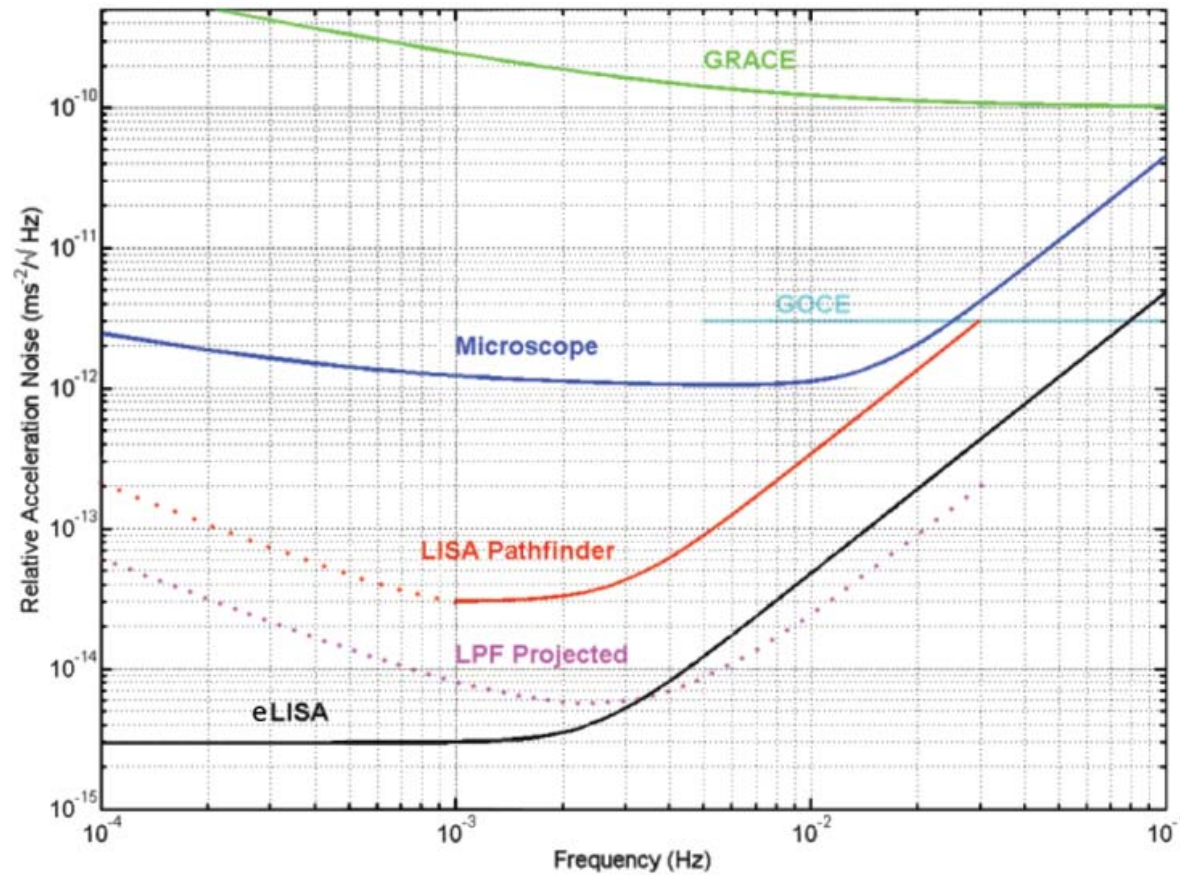
Inside their housings, the test masses collide with some of the few gas molecules still present. This noise term becomes smaller with time, as more gas molecules are vented to space.



Sensing noise

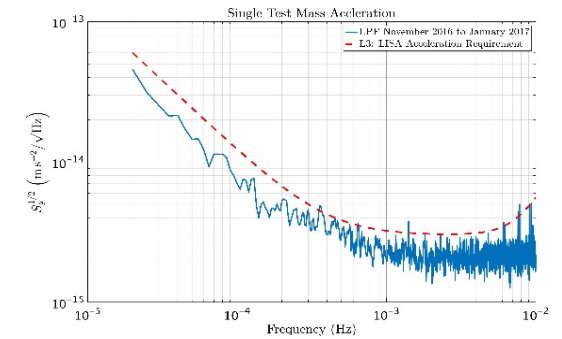
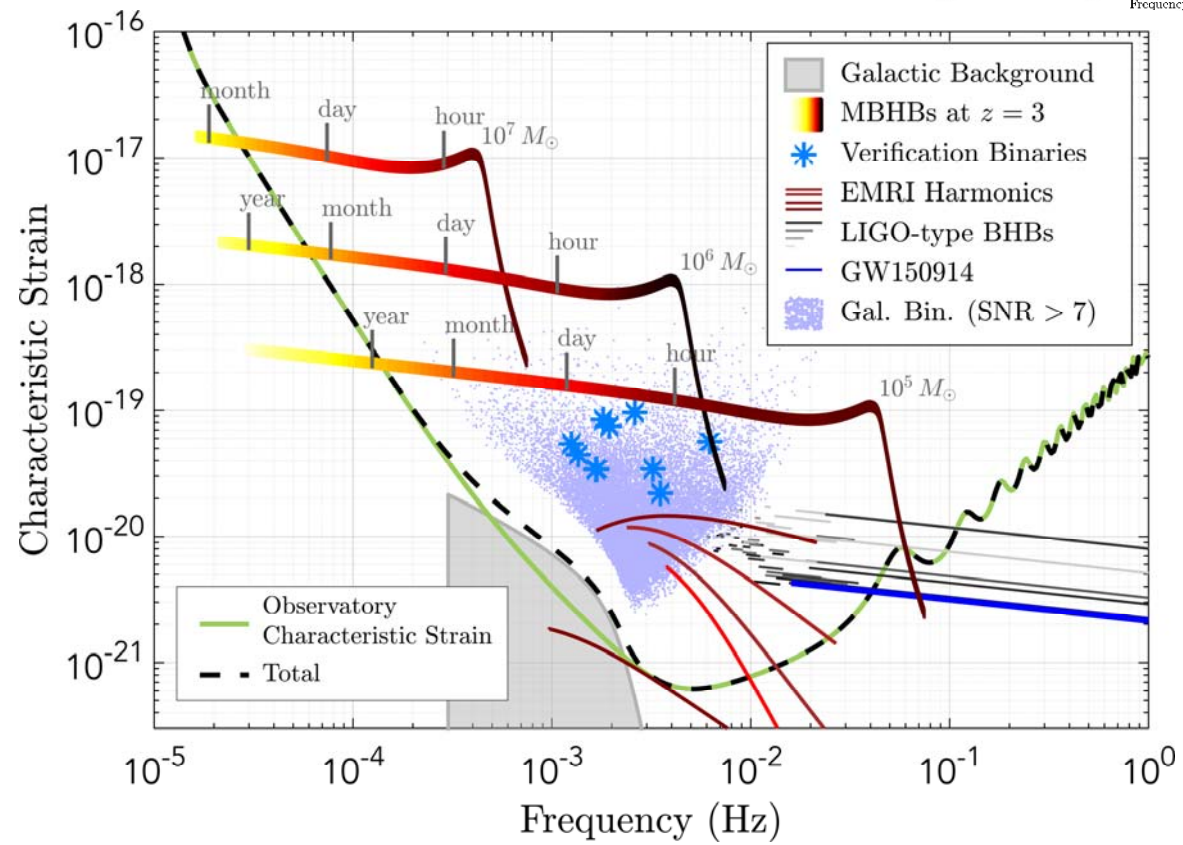
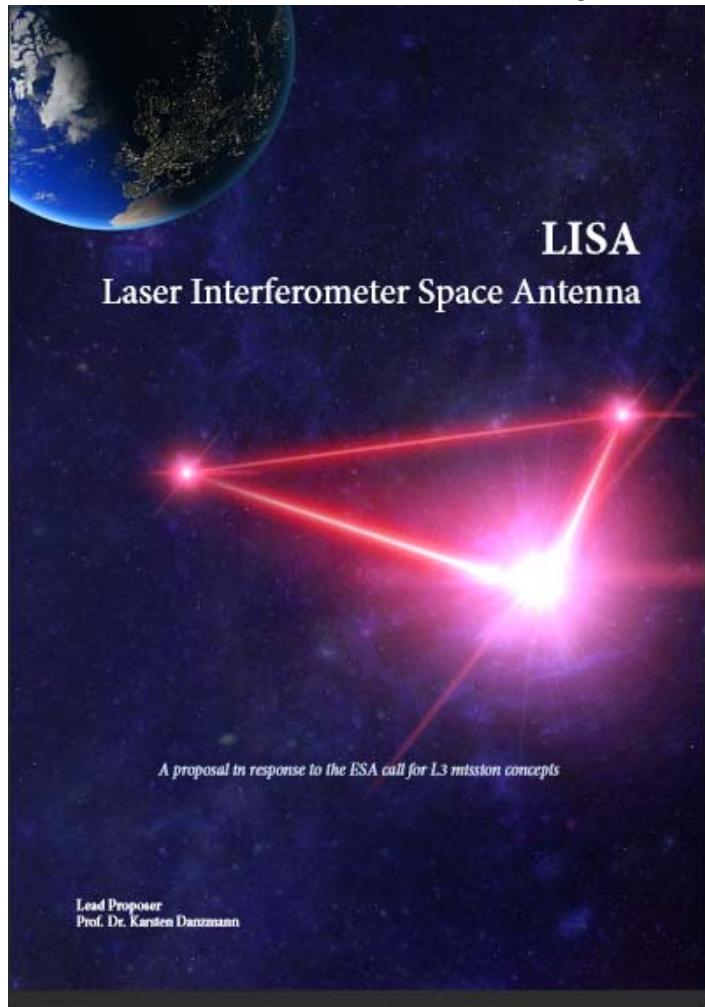
The sensing noise of the optical metrology system used to monitor the position and orientation of the test masses, at a level of 35 fm / √Hz, has already surpassed the level of precision required by a future gravitational-wave observatory by a factor of more than 100.

LISA Pathfinder (LISA Technology Demonstrator)

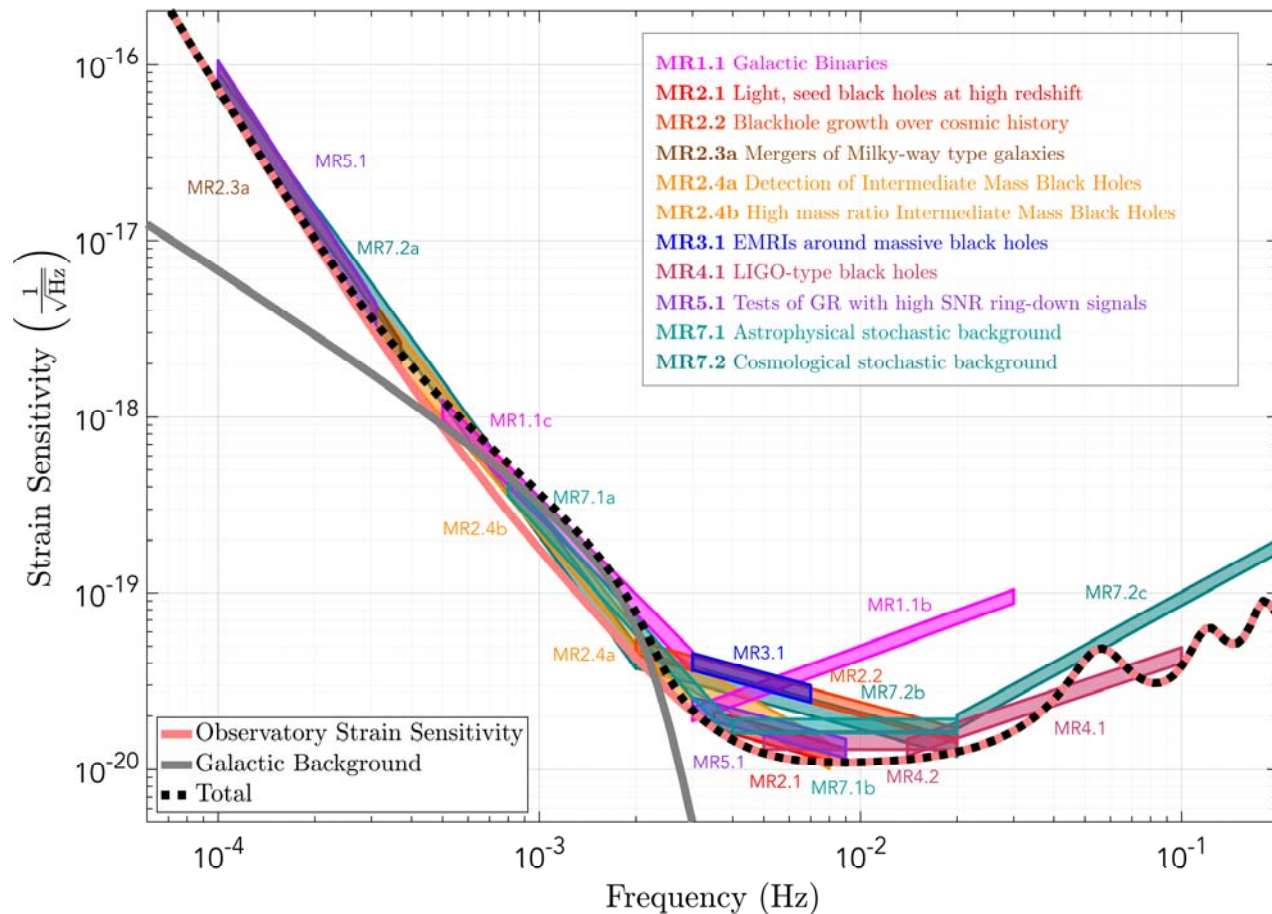


QTSpace, 26-31 Mar 2017, Malta

LISA (Laser Interferometer Space Antenna)



LISA (Laser Interferometer Space Antenna)



QTSpace, 26-31 Mar 2017, Malta

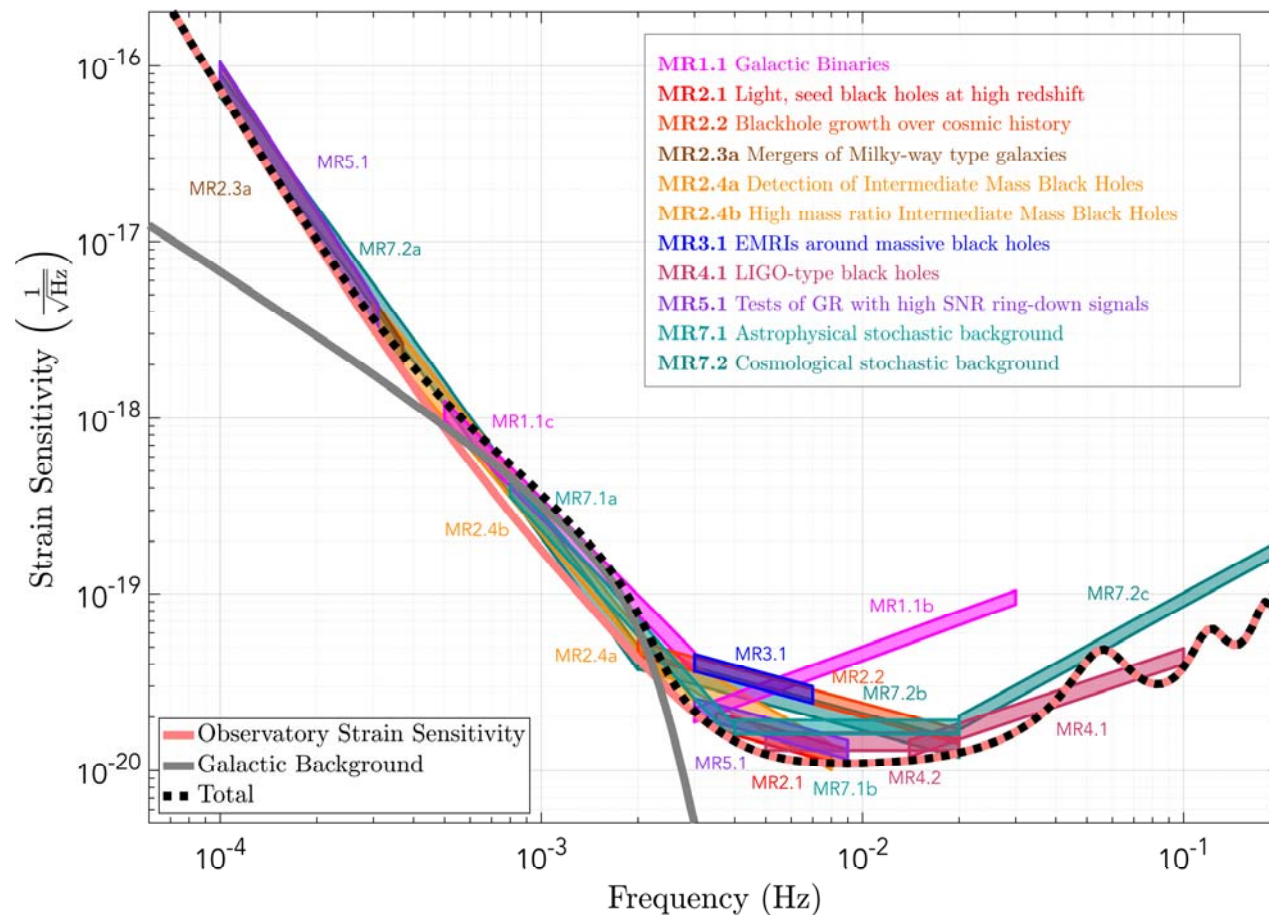
SI2.2: Study the growth mechanism of MBHs from the epoch of the earliest quasars

OR2.2.a Have the capability to detect the signal for coalescing MBHs with mass $10^4 < M < 10^6 M_\odot$ in the source frame at $z \lesssim 9$. Enable the measurement of the source frame masses at the level limited by weak lensing (5 %).

OR2.2.b For sources at $z < 3$ and $10^5 < M < 10^6 M_\odot$, enable the measurement of the dimensionless spin of the largest MBH with an absolute error better than 0.1 and the detection of the misalignment of spins with the orbital angular momentum better than 10 degrees. This parameter accuracy corresponds to an accumulated SNR (up to the merger) of at least ~ 200 .

MR2.2: The most stringent requirement is set by being able to measure the spin of a threshold system with total intrinsic mass of $10^5 M_\odot$, mass ratio of $q = 0.2$, located at $z = 3$. This will satisfy both OR2.1.a and 2.1.b. Achieving an SNR of 200 requires a strain sensitivity of $4 \times 10^{-20} \text{ Hz}^{-1/2}$ at 2 mHz and $1.3 \times 10^{-20} \text{ Hz}^{-1/2}$ at 20 mHz. All systems in OR2.2.a and 2.2.b with higher mass, mass ratios, spins, or lower redshift will result in higher SNR, and better spin estimation.

LISA (Laser Interferometer Space Antenna)



QTSpace, 26-31 Mar 2017, Malta

SI5.1 Use ring-down characteristics observed in MBHB coalescences to test whether the post-merger objects are the black holes predicted by GR.

OR5.1 Have the ability to detect the post-merger part of the GW signal from MBHBs with $M > 10^5 M_\odot$ out to high redshift, and observe more than one ring-down mode to test the “no-hair” theorem of GR.

MR5.1: The range of systems defined in OR5.1 sets a constraint on the sensitivity curve by requiring the high SNR and the observation of the merger. For masses at the low end of the range, the threshold system is one out at $z = 15$ with a mass of $10^5 M_\odot$, which will give an SNR of ~ 100 in the ringdown if the strain sensitivity is better than $2 \times 10^{-20} \text{ Hz}^{-1/2}$ at 3 mHz and $1 \times 10^{-20} \text{ Hz}^{-1/2}$ at 9 mHz. The contours of SNR in the mass/redshift plane are complicated, but we can constrain a point on the high mass end by considering a system of $10^7 M_\odot$ out at redshift 4. This system constrains the strain sensitivity to be better than $7 \times 10^{-17} \text{ Hz}^{-1/2}$ at 0.1 mHz, and $3 \times 10^{-18} \text{ Hz}^{-1/2}$ at 0.3 mHz, with the goal to extend this sensitivity down to low frequencies to see more of the inspiral phase, and allow earlier detection. Systems with masses between these two end points are considered ‘Golden’ binaries, yielding SNRs of up to 1000 for systems out to redshift 3.

LISA (Laser Interferometer Space Antenna)

SI5.2 Use EMRIs to explore the multipolar structure of MBHs

OR5.2: Have the ability to detect ‘Golden’ EMRIs (those are systems from OR3.1 with $\text{SNR} > 50$, spin > 0.9 , and in a prograde orbit) and estimate the mass of the SOBH with an accuracy higher than 1 part in 10^4 , the mass of the central MBH with an accuracy of 1 part in 10^5 , the spin with an absolute error of 10^{-4} , and the deviation from the Kerr quadrupole moment with an absolute error of better than 10^{-3} .

MR5.2: The MRs are the same as MR3.1, but due to uncertainties in the astrophysical populations, a mission lifetime of several years is essential here to increase the chance of observing a Golden EMRI.

SI5.3 Testing for the presence of beyond-GR emission channels

Test the presence of beyond-GR emission channels (dipole radiation) to unprecedented accuracy by detecting GW150914-like binaries, which appear in both the LISA and LIGO frequency bands [15]. The ORs and MRs are the same as those in SI4.1.

SI5.4 Test the propagation properties of GWs

Test propagation properties of GW signals from EMRIs and from coalescing MBHBs. Detect the coalescence of Golden MBHBs (those systems described in OR2.2 with an $\text{SNR} > 200$) and have the ability to detect a Golden EMRI (as defined in OR5.2) which allows us to constrain the dispersion relation and set upper limits on the mass of the graviton and possible Lorentz invariance violations. The ORs and MRs are the same as those in MR2.2 and MR3.1.

SI5.5 Test the presence of massive fields around massive black holes with masses $> 10^3 M_\odot$

Constrain the masses of axion-like particles or other massive fields arising in Dark-Matter models by accurately measuring the masses and spins of MBHBs [16]. The requirements on the accuracy of the mass and spin measurements are the same as in SI2.2.

Investigate possible deviations in the dynamics (encoded in the GW signal) of a solar mass object spiralling into an intermediate mass BH (mass $< a\text{few}10^4 M_\odot$) due to the presence of a Dark Matter mini-spike around the IMBH [17]. This is a discovery project and the high frequency requirements stated in MR4.1, MR4.2 make such a discovery possible.

Summary

- Space is an obvious environment for carrying out fundamental physics experiments.
- The first pioneering experiments are showing technologies are now available for high-precision experiments exceeding ground-based capabilities.
- The work-horse at the moment is the use of macroscopic proof-mass type instruments.
- The potential return from improved sensitivities with new technologies is enormous and there are some complementary science goals.